JOURNAL OF CATALYSIS 118, 53–67 (1989)

A Multicomponent, Multilayer Model of Surface Segregation in Alloy Catalysts

JOHN K. STROHL AND TERRY S. KING

Department of Chemical Engineering, Iowa State University, 231 Sweeney Hall, Ames, Iowa 50011-2230

Received July 12, 1988; revised February 20, 1989

A model for the quantitative prediction of surface segregation in alloy systems is presented. A chemical thermodynamic approach is used in the development of the model, and a multilayer surface region is assumed. Features of this model include multicomponent capability (the components may be different sizes) and the ability to use virtually any mixing model. Surface free energy data are incorporated and no adjustable parameters are needed. The modeling method is discussed in detail with examples given for the Ag–Au, Cu–Ni, and Au–Ni binary systems and the Cu–Ni–Pt ternary system. Both regular and Margules solution models were used, but the Margules model agreed more closely with experimental data for the Cu–Ni system. The segregating element in the Au–Ni binary was found to be gold. Greater segregation of gold and better agreement with experimental data resulted when the size differences between the elements were accounted for. In the Cu–Ni–Pt system, copper was predicted to segregate to the surface, causing a relative depletion of both nickel and platinum in the first atomic layer. The second layer was enriched in platinum and depleted in both nickel and copper.

INTRODUCTION

The understanding of the composition, structure, and behavior of surfaces is extremely important in a wide variety of disciplines. Catalysis is just one of the areas in which knowledge of surfaces is crucial in obtaining an overall understanding of phenomena occurring at the surface. If one desires to predict the composition of the surface of a mixture (either liquid or solid), then it is necessary to understand the phenomenon of surface segregation. Surface segregation refers to the appearance of atomic or molecular species in a greater concentration at a surface than is present in the bulk of the material.

It has been known for quite some time that alloying of an active catalyst metal with, for example, a metal that is not catalytically active can alter catalytic behavior in ways not obvious from the individual behavior of the two metals (*1–4*). Various electronic and structural reasons have been given to explain such effects (*4*) but in all cases the surface composition plays an important role in the proposed explanations. In addition, composition in the near surface region may be responsible for catalytic effects that are not directly attributable to the surface layer composition. For example, two investigations have observed a significant variation in the electronic structure near the fermi level of copper when copper is deposited in a monolayer on ruthenium (*5, 6*). Presumably, significant electron transfer occurs from ruthenium to copper states. In some systems subsurface adsorption, particularly of hydrogen, has been observed (*7–10*). The weakly adsorbed, subsurface adsorption state may be involved in catalytic reactions (*11*). For a mixture of metals, the subsurface adsorption state may be significantly influenced by the composition in the second and lower layers.

The first person to lay the theoretical groundwork for the prediction of surface segregation was J. W. Gibbs (*12*) who used the postulates of classical thermodynamics to derive the equation

$$\Gamma_A = -(\partial\sigma/\partial\mu_A)_{T,P}. \quad (1)$$

0021-9517/89 $3.00

In the above expression, commonly known as the Gibbs adsorption isotherm equation, Γ_A represents the surface excess of component A in an A–B binary, σ the surface tension, and μ_A the chemical potential of A. The surface excess is defined by the relation

$$\underline{A}\Gamma_i = N_i^{\text{Tot}} - (N_i^{\alpha} + N_i^{\beta}),$$

where $\underline{A}$ is the interfacial area, N_i^{Tot} is the number of total moles of i in the system, and N_i^{α} and N_i^{β} represent the number of moles of i in phases α and β, respectively, if one assumes that the concentration of i in these phases remains constant and equal to the bulk values up to the imaginary dividing surface. Qualitatively, Eq. (1) says that if an increased amount of A tends to lower the surface tension of the solution, then component A should be found in excess within the surface region.

Although Eq. (1) is thermodynamically rigorous, it is not in a form that allows one to readily calculate surface compositions given only overall concentrations, temperature, and pressure. Since the time of Gibbs, therefore, much effort has been expended in developing models for predicting surface segregation that use easily measurable or obtainable data. These surface segregation models differ from one another mainly in the assumptions used regarding the thickness of the surface region (i.e., how many atomic or molecular layers at the interface are allowed to vary in composition from the bulk of the material) and in the manner in which solution behavior is characterized. Assuming that the surface region consisted of only the outermost layer of atoms or molecules, Butler (*13*) in 1932 defined chemical potentials in the surface region by using activity expressions analogous to those used in bulk systems,

$$\mu_A^S = \mu_A^{S,0} + RT \ln a_A^S, \qquad (2)$$

where μ_A^S is the chemical potential of A in the surface region, $\mu_A^{S,0}$ the pure component surface chemical potential, and a_A^S the activity of A in the surface layer. Using the assumptions of a monolayer surface region, ideal solution behavior, and equal molar surface areas of constituents, Shuchowitzky (*14*) derived the following expression for the prediction of surface segregation in binary systems:

$$X_a'/X_b' = (X_a^{\beta}/X_b^{\beta}) \times \exp[A(\sigma_b - \sigma_a)/RT]. \qquad (3)$$

In this expression, X_a' and X_b' represent the first-layer mole fractions of components A and B, respectively; X_a^{β} and X_b^{β} represent the respective bulk mole fractions; A represents the molar area of the components; and σ_a and σ_b represent the pure component surface tensions of A and B. Guggenheim (*15*), in an effort to incorporate more complex solution behavior, assumed regular solution behavior and used a statistical thermodynamic approach in developing equations for predicting surface segregation in the monolayer region. Defay and Prigogine (*16*) showed that the Guggenheim model, while accurate for some systems, was fundamentally incorrect because it failed to meet the rigorous thermodynamic criterion expressed in the Gibbs adsorption isotherm equation. In order to come closer to meeting this criterion while still assuming regular solution behavior, Defay and Prigogine allowed for the outermost two atomic or molecular layers of a solution to differ in composition from the bulk. The logical limit to the regular solution surface segregation model for binary systems composed of molecules of equal surface areas was reached by Ono and co-workers (*17*). They used a statistical thermodynamic approach to derive a model that contains an infinite number of layers in the surface region and that is consistent with the Gibbs adsorption isotherm. A semiclassical thermodynamic technique was used by Mezey and Giber (*18*) in developing a multilayer surface segregation model. They derived an equilibrium criterion by performing a constrained minimization on an expression for total Gibbs energy. An expression for the

chemical potential of the surface region was then postulated.

Numerous techniques, in addition to those described above, have been proposed (*19–33*) for predicting surface segregation in binary systems. Despite the relatively great number of methods that have been used to predict surface segregation, there is still a need for a rigorous model general enough to account for segregation behavior in multilayer systems containing three or more constituents and to account for any size differences between components in a rigorous fashion. Ternary and higher alloys have received little attention in spite of their increased use as catalysts. A model that utilizes surface free energy data to account for bonding energy differences between surface and bulk components is also needed. For example, some of the so-called broken-bond models (Ref. (*20*)) use only bulk data to figure the differences between bulk and surface bond strengths. In this paper we present such a multilayer, multicomponent model and demonstrate how it can be used to predict surface segregation in alloy systems of catalytic importance.

THEORY

The derivation of the multilayer, multicomponent surface segregation model begins by assuming a semi-infinite solid with a planar surface comprising a series of atomic layers l numbered in ascending order in the direction from the outer surface towards the bulk region. The fundamental equation for layer l in a system composed of m distinct chemical species can then be written as

$$\underline{G}^l = f(T, P, A^l, N_1^l, N_2^l, \ldots, N_m^l, N_1^{l-1}, N_2^{l-1}, \ldots, N_m^{l-1}, N_1^{l+1}, N_2^{l+1}, \ldots, N_m^{l+1}), \quad (4)$$

where $\underline{G}^l$ is the total Gibbs energy of layer l, $\underline{A}^l$ is the total area of layer l, and the N_i^l, N_i^{l-1}, N_i^{l+1} terms represent the mole numbers of component i in layer l, $l-1$, and $l+1$, respectively. Since the model developed assumes that nearest-neighbor interactions are important, the mole numbers of components in the layers adjacent to the layer l are included in Eq. (4). Using the method of Legendre transforms (*34*), one may express the total differential of (4) at constant temperature and pressure as

$$\mathrm{d}\underline{G}^l = \sigma^l \mathrm{d}\underline{A}^l + \sum_i \mu_i^l \mathrm{d}N_i^l + \sum_i \left(\frac{\partial \underline{G}^l}{\partial N_i^{l-1}}\right)_{T,P,\underline{A}^l,N_j \neq N_i^{l-1}} \mathrm{d}N_i^{l-1} + \sum_i \left(\frac{\partial \underline{G}^l}{\partial N_i^{l+1}}\right)_{T,P,\underline{A}^l,N_j \neq N_i^{l+1}} \mathrm{d}N_i^{l+1}, \quad (5)$$

where

$$\sigma^l = \left(\frac{\partial \underline{G}^l}{\partial \underline{A}^l}\right)_{T,P,N_i^l} \quad \text{and} \quad \mu_i^l = \left(\frac{\partial \underline{G}^l}{\partial N_i^l}\right)_{T,P,\underline{A}^l,N_j \neq N_i^l}.$$

Writing $\mathrm{d}\underline{A}^l$ in terms of partial molar areas ($\overline{A}_i^l$) gives

$$\mathrm{d}\underline{A}^l = \sum_i \overline{A}_i^l \mathrm{d}N_i^l. \quad (6)$$

Substituting (6) into (5) and rearranging yields

$$\mathrm{d}\underline{G}^l = \sum_i (\sigma^l \overline{A}_i^l + \mu_i^l)\mathrm{d}N_i^l + \sum_i \left(\frac{\partial \underline{G}^l}{\partial N_i^{l-1}}\right)_{T,P,\underline{A}^l,N_j \neq N_i^{l-1}} \mathrm{d}N_i^{l-1} + \sum_i \left(\frac{\partial \underline{G}^l}{\partial N_i^{l+1}}\right)_{T,P,\underline{A}^l,N_j \neq N_i^{l+1}} \mathrm{d}N_i^{l+1}. \quad (7)$$

From (7) one can immediately write

$$\left(\frac{\partial \underline{G}^l}{\partial N_i^l}\right)_{T,P,N_j \neq N_i^l} = \sigma^l \overline{A}_i^l + \mu_i^l. \quad (8)$$

Using Eq. (8) to define a surface chemical potential δ_i^l in a form analogous to that of bulk chemical potential allows one to write

$$\left(\frac{\partial \underline{G}^l}{\partial N_i^l}\right)_{T,P,N_j \neq N_i^l} = \delta_i^l \equiv \delta_i^{0,l} + RT \ln a_i^l, \quad (9)$$

where a_i^l is the surface activity of component i in layer l and $\delta^{0,l}$ is the pure component surface chemical potential of i in layer l. Because under equilibrium conditions the chemical potential of component i in the bulk region must be equal to the chemical potential in layer l,

$$\mu_i^l = \mu_i^\beta = \mu_i^{0,\beta} + RT \ln a_i^\beta \quad \text{(equilibrium)}, \quad (10)$$

where the β superscripts indicate the bulk region and $\mu_i^{0,\beta}$ is the pure component bulk chemical potential of i. Substituting (9) and (10) into (8) yields

$$\delta_i^{0,l} - \mu_i^{0,\beta} + RT \ln \left(\frac{a_i^l}{a_i^\beta}\right) = \sigma^l \bar{A}_i^l. \quad (11)$$

Because the above equation must hold for all compositions, for pure i the relation in (11) becomes

$$\delta_i^{0,l} - \mu_i^{0,\beta} = \sigma_i^l A_i^l, \quad (12)$$

where A_i^l is the molar area of pure component i in layer l and similarly σ_i^l is the surface free energy of pure component i in layer l. Substituting (12) into (11) and rearranging give

$$\sigma^l = \sigma_i^l \frac{A_i^l}{\bar{A}_i^l} + \frac{RT}{\bar{A}_i^l} \ln \left(\frac{a_i^l}{a_i^\beta}\right). \quad (13)$$

In general, for a system containing m chemical species, m equations of the form given in (13) may be written for a given atomic layer. Eliminating the common variable σ^l results in a set of $m - 1$ independent equations per layer. If one desires to calculate composition profiles from these equations, it is necessary to express the unknown variables in terms of the constituent mole fractions present in each layer. Thus, for a system comprising l atomic or molecular layers, the net result is a system of $l(m - 1)$ independent, nonlinear equations with $l(m - 1)$ unknowns (the independent mole fractions of the species in the different layers). The equilibrium composition profile is therefore determined by the set of mole fractions satisfying this system of equations. If one starts with Eq. (13) and makes the appropriate assumptions (monolayer surface region, ideal solution behavior, equal and constant molar areas), the result for a binary system is the same as given in Eq. (3).

Two terms that must be expressed in terms of composition in (13) are the partial molar area term $\bar{A}_i^l$ and the surface activity term a_i^l. The partial molar areas may be stated in terms of mole fractions either by proposing a functional relation or by obtaining actual atomic area versus composition data and differentiating. In order to express the nonlinear term containing the surface activity in terms of mole fractions, it is first necessary to make several assumptions. If one assumes that the energy of an alloy crystal can be modeled by the atoms in the crystal being connected to each other by chemical bonds that are characteristic of the two atoms participating in the bond, and if one assumes that the energetic state of a given atom can be described by only taking into account nearest-neighbor interactions, then the activity of a species in an atomic layer must be a function of the composition in that layer and in the two adjacent layers. Note that Swalin (*35*) refers to this description as a quasi-chemical model. However, Guggenheim (*38*) and subsequently others have used the term quasi-chemical to mean a specific, nonrandom mixing model. To avoid confusion we will use the term chemical model to refer to the bond model described above. Mathematically, this may be stated as

$$a^l = f[(x_1^l, x_2^l, \ldots, x_{m-1}^l), (x_1^{l-1}, x_2^{l-1}, \ldots, x_{m-1}^{l-1}), (x_1^{l+1}, x_2^{l+1}, \ldots, x_{m-1}^{l+1})], \quad (14)$$

where terms of the form $x_i^{(k)}$ represent the mole fractions of species i in layer k. Equation (14) thus serves as a means of coupling the equations given in (13). The assumptions regarding nearest-neighbor-only interactions have been shown by the use of various potential models (*36, 37*) to be rea-

sonable for FCC systems. In the case of an A–B binary alloy system where random-mixing, regular solution behavior is assumed, it can be shown that

$$RT \ln(a_B^l) = (N_0\omega_{AB}/Z)\{Z_L(x_A^l)^2 + Z_v[(x_A^{l-1})^2 + (x_A^{l+1})^2]\} + RT \ln(x_B^l), \quad (15)$$

where N_0 is Avogadro's number and Z, Z_L, and Z_v are the total, lateral, and vertical coordination numbers, respectively (see Appendix for derivation). The term ω_{AB} in (15) is the "regular solution parameter" and is defined by the relation

$$\omega_{AB} \equiv Z[U_{AB} - \tfrac{1}{2}(U_{AA} + U_{BB})], \quad (16)$$

where U_{AA}, U_{BB}, and U_{AB} are bulk bond energies. In practice, values for ω_{AB} may be calculated from excess free energy of mixing data (*34*) by using the relation

$$N_0\omega_{AB} = \Delta G^{ex}/x_A x_B. \quad (17)$$

As noted in the Appendix, Eq. (15) is an approximation that allows one to write the surface activity concisely without introducing significant error. Surface region models that suggest an activity expression different from that given above have been previously postulated (*18, 19*).

In a fashion similar to that of the two-component case, the surface activity for a multicomponent, regular solution system can be written as

$$RT \ln a_i^l = N/Z \left\{ Z_L \left[(1 - x_i^l) \sum_j \omega_{ij} x_j^l - \sum_j \sum_k \omega_{jk} x_j^l x_k^l \right] + Z_v \left[(1 - x_i^{l-1}) \sum_j \omega_{ij} x_j^{l-1} - \sum_j \sum_k \omega_{jk} x_j^{l-1} x_k^{l-1} \right] + Z_v \left[(1 - x_i^{l+1}) \sum_j \omega_{ij} x_j^{l+1} - \sum_j \sum_k \omega_{jk} x_j^{l+1} x_k^{l-1} \right] \right\} + RT \ln x_i^l. \quad (18)$$

One can take two approaches to extend the binary and ternary activity models to more realistic mixtures. The detailed, microscopic models used to derive Eqs. (15) and (18) can be made more complex so that nonrandom mixing (*35, 38*) is described. In addition, the pairwise-interaction method can be abandoned in favor of a model incorporating three-center or four-center bonding groups (*38*). With these approaches the complexity of the models quickly escalates, yet they are often still deficient in their ability to describe the mixing behavior of real systems.

Another approach is to recognize that various terms in Eqs. (15) and (18) are defined as activity coefficients of individual layers. One can then generalize from an activity coefficient for a regular solution model to one for a general, empirical model. For example, the term $N_0\omega_{AB}(x_A^l)^2$ is a portion of the activity coefficient of A in layer l when a regular solution model is assumed. If we assume that the form of Eq. (15) holds for an arbitrary, real mixture we can write the general form of the activity of species i in a binary as

$$RT \ln (a_i^l) = RT \ln\{1/Z[Z_L\gamma_i^l + Z_v(\gamma_i^{l-1} + \gamma_i^{l+1})]\} + RT \ln(x_i^l), \quad (19)$$

where the terms γ_i^l, γ_i^{l-1}, and γ_i^{l+1} represent the activity coefficients of component i associated with the l, $l-1$, and $l+1$ layers, respectively. By making this generalization of the activity coefficients from the random, regular solution model to the empirical case, we are taking the same approach as is often used in bulk solution thermody-

namics. It allows the use of experimental values or empirical models of activity coefficients. Consequently, nonrandom, nonregular solutions can be modeled if the mixing properties of the alloy are known.

The activity models derived above are different from the model proposed by Mezey and Giber (*18*) in which the authors multiply the bulk-type activity contributions of the adjacent layers by a factor α instead of the ratio of vertical bonds to total bonds. In analogous fashion, Mezey and Giber assign the coefficient $(1 - 2\alpha)$ to the lateral component of the surface activity instead of the ratio of lateral to total coordination. The factor α is an empirically determined parameter that in essence attempts to account for long-range atomic interactions and subtleties involving the nature of metal-to-metal bonding. Mezey and Giber treat α as a constant for a given alloy system (α is set equal to the arithmetic average of the pure-component α terms) and use it in all the surface activity expressions, regardless of the atomic layer. Such a usage is inappropriate, however, because in calculating α, pure component data for σ are used:

$$\alpha_i^0 = \sigma_i^0 A_i^0 / \Delta G_{a,i}^*. \tag{20}$$

In the above expression α_i^0 is the value of α for pure i, $\sigma_i^0 A_i^0$ the pure component product of σ and molar area, and $\Delta G_{a,i}^*$ the molar Gibbs energy of atomization. Note, however, that the differences between bond energies of fully coordinated atoms and atoms with less than full coordination partially comprise the σ_i^0 term. Since bond energies vary with coordination, the use of α for layers whose atoms are all fully coordinated (i.e., atoms in all atomic layers but the first) is not appropriate. Another point of confusion arising from the Mezey and Giber model results from their definition of a surface excess chemical potential $\mu_i^{s,l}$. This term is not an excess quantity in the usual sense; it does not equal zero for an ideal solution because it contains the product of pure component surface free energy and pure component molar area:

$$\mu_i^{s,l} = RT \ln \gamma_i^l + \sigma_i^l A_i^l. \tag{21}$$

On the other hand, the bulk excess chemical potential defined by the authors does equal zero for an ideal solution. These definitions necessarily force all contributions of the surface free energy of the pure component contributions to the first layer. Although this approximation is a reasonable one, these definitions of excess chemical potential result in the inappropriate use of α to describe interlayer interactions other than the first.

SOLUTION OF THE MULTILAYER, MULTICOMPONENT EQUATIONS

The algorithm used to solve the set of equations of the form given in (13) is essentially one of multivariable successive substitution. Initially, all the layers in the surface region (arbitrarily chosen to be 20 layers deep for the results shown below) are assumed to be of the same composition as the bulk region. Beginning with the outermost layer, values of σ are computed in reference to each component present in the system. A weighted average value of the layer surface tension $\hat{\sigma}^l$ is then determined by the expression

$$\hat{\sigma}^l = \sum_i x_i^l \sigma^l, \tag{22}$$

where σ^l is the value calculated for each species i with the current values of the variables on the right-hand side of Eq. (13). New values of x_i^l are then generated by replacing σ^l in (13) by $\hat{\sigma}^l$ and solving for x_i^l:

$$x_i^l = \left(\frac{a_i^\beta}{1/Z[Z_L \gamma_i^l + Z_v(\gamma_i^{l-1} + \gamma_i^{l+1})]}\right) \exp\left\{\frac{\bar{A}_i^l \hat{\sigma}^l - A_i^l \sigma_i^l}{RT}\right\}. \tag{23}$$

Note that the right-hand side in the above expression is still determined by use of the previous compositions. The term σ_i^l in (23) and (13) is taken to be equal to the pure component surface free energy for the out-

ermost layer and zero elsewhere. This approximation is in keeping with the nearest-neighbor-interaction philosophy of the activity model.

After all of the mole fractions in a given layer have been updated, the above process of revising composition is repeated for the next deeper layer. After the deepest layer is reached, the convergence criterion is checked; if it is not found to be satisfactory, the entire procedure is repeated starting from the first layer. The convergence criterion requires that the updated values for mole fractions differ negligibly from the old values. When the criterion is met, the equilibrium conditions expressed by (13) are satisfied, and the final values of the mole fractions of all the layers constitute the equilibrium composition profile. The main advantages of this algorithm are that it correctly incorporates surface free energy data (which in effect allows the bond energies of the surface atoms to differ from bond energies in the bulk state), it allows for great flexibility in choosing an activity model, it permits multicomponent alloys to be modeled, and it directly accounts for size differences between components. It does not allow the mixing properties in the surface region (i.e., ω_{AB}) to differ from the bulk mixing properties. This is a limitation due to lack of empirical data rather than due to the model itself.

The above model and algorithm can also be applied to liquid mixtures as well if one assumes a quasi-crystalline structure (*38*). After calculating the liquid surface composition by using the above technique, one can calculate the mixture surface tension directly from the set of equations given by (13).

RESULTS AND DISCUSSION

Results of calculations using the above algorithm are presented for Ag–Au, Cu–Ni, and Au–Ni binary systems and for the Cu–Ni–Pt ternary system. Activity coefficients were determined by use of either the regular solution model (see Eqs. (15) and (18)) or the empirical (nonrandom) three-suffix Margules model given by

$$RT \ln \gamma_1 = (A + 3B)(x_2)^2 - 4B(x_2)^3$$
$$RT \ln \gamma_2 = (A - 3B)(x_1)^2 + 4B(x_1)^3, \quad (24)$$

where the constants A and B are determined from activity data at infinite dilution. Atomic areas were obtained from lattice constants by use of the relations

$$A_{100} = a_0^2/2; \quad A_{111} = a_0^2\sqrt{3}/4, \quad (25)$$

where a_0 is the lattice constant and A_{100} and A_{111} are the pure-component atomic areas for the (100) and (111) surfaces, respectively. Data for lattice constants were taken from Ref. (*39*). Unless otherwise noted, lattice constants were assumed to be linear functions of composition, a common observation for many alloy systems (*39*). Lattice spacing relaxation at the surface is ignored. This is a good approximation for a (111) or (100) orientation but may be incorrect for other orientations. Surface free energy data for all the elements studied were obtained from Refs. (*40*) and (*41*), while data used in calculating regular solution parameters and Margules constants were taken from Hultgren *et al.* (*42*). Examples of some of the values of the parameters used in the computations are listed in Table 1.

The surface segregation model described in the above paragraphs requires data for the surface free energy, heat of mixing, and molar area of the pure component. Of these, the most difficult to obtain experimentally are surface free energy data for

TABLE 1

Molar Areas and Surface Free Energies

Element	A ($\times 10^{-8}$ cm^2/mole)[a]	σ ($\times 10^5$ cal/cm^2)
Ag	5.04	3.07 (550 K)
Au	5.01	3.61 (550 K)
Cu	3.95	3.86 (1100 K)
Ni	3.73	5.03 (1100 K)
Pt	4.63	6.14 (1100 K)

[a] (100) surface, 298 K.

solid metals. Therefore, it may be necessary in some cases to resort to methods of estimating the surface free energy of a pure, solid metal. One such method is the correlation for cubic metals given by Murr (*41*),

$$\sigma_T \cong 1.2\sigma_{T_m} + 0.45(T_m - T), \quad (26)$$

where σ_T is the surface free energy of the solid (in ergs/cm^2) at temperature T and σ_{T_m} is the surface tension of the liquid metal at the melting temperature T_m. Data for σ_{T_m} have been compiled for virtually all metals of catalytic importance and are readily available (*41*). Another correlation, given by Tyson (*40*), makes use of heat of sublimation data:

$$\sigma_T A = k\Delta H_0^{Sub} - RT. \quad (27)$$

In the above expression, A represents the pure component molar area at temperature T, and ΔH_0^{Sub} represents the heat of sublimation of the metal at 0 K. The heat of sublimation data may be obtained from such references as Hultgren *et al.* (*43*) or Kittel (*44*). The parameter k is empirically determined; for the (111) and (100) surfaces of an FCC metal, typical values of k are 0.17 and 0.20, respectively.

If heat of mixing data for a metallic system cannot be obtained from a published source containing experimentally determined values (e.g., Hultgren *et al.* (*42*)), one must turn to sources that use theoretical techniques to predict such values. One such source is the paper by Miedema (*45*)

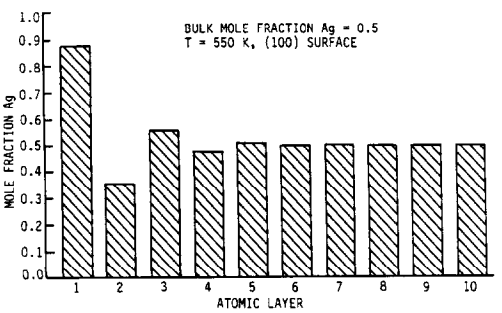

FIG. 1. Surface region composition depth profile for the Ag–Au system.

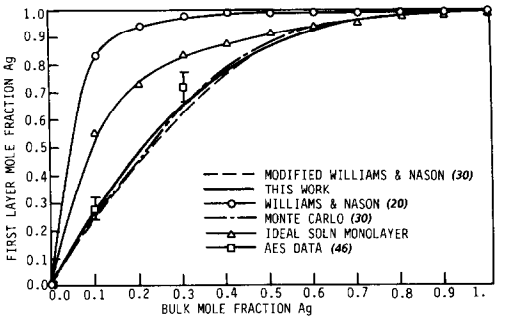

FIG. 2. Comparison of other predictions for the surface segregation of silver in the Ag–Au system with this work and AES data.

that outlines an electronic model for the prediction of heats of formation for alloys. A useful table summarizing the heats of formation for all possible (binary) 1 : 1 transition metal alloys is presented in this reference.

Ag–Au System

The Ag–Au system was chosen to illustrate the surface behavior of an exothermic alloy and to serve as a comparison to previous models and to experimental results. A typical composition depth profile for the Ag–Au alloy is shown in Fig. 1. The "damped oscillatory" behavior of Ag composition seen in this figure has been noted before (*30*) and is due to the exothermic heat of mixing exhibited by this system; since unlike atoms prefer to be adjacent to one another in an exothermic system, the relative abundance of Ag in the first layer results in a relative abundance of Au in the second atomic layer. Table 2 is a comparison of a composition depth profile for the Ag–Au alloy determined with the methods described in this paper with profiles computed with the Monte Carlo simulation technique and Auger electron spectroscopy data (*30, 46*). Note that although the Monte Carlo technique is completely different from the multilayer model described here, the agreement between the results is very good. Figure 2 is a comparison of predicted first-layer silver composition of the Ag–Au

TABLE 2

Comparision of Ag–Au Depth Profiles from this Work to Profiles Computed by Use of the Monte Carlo Simulation Technique (*30*) and to AES Data (*46*) Where Available

X_{Ag} (bulk)	Layer	This work X_{Ag}	Monte Carlo technique X_{Ag}	AES X_{Ag}
0.3	1	0.67	0.68	0.72 ± 0.06
T = 550 K	2	0.19	0.21	0.20 ± 0.10
	3	0.34	0.39	
	4	0.29	0.29	
	5	0.30	0.30	
	6	0.30	0.30	
0.3	1	0.62	0.64	0.60 ± 0.07
T = 650 K	2	0.21	0.22	0.24 ± 0.11
	3	0.33	0.34	
	4	0.29	0.30	
	5	0.30	0.30	
	6	0.30	0.30	
0.3	1	0.59	0.61	0.61 ± 0.10
T = 750 K	2	0.23	0.25	0.26 ± 0.15
	3	0.32	0.31	
	4	0.30	0.30	
	5	0.30	0.30	
	6	0.30	0.30	
0.5	1	0.88	0.88	
T = 500 K	2	0.36	0.36	
	3	0.56	0.56	
	4	0.48	0.48	
	5	0.51	0.51	
	6	0.50	0.50	
0.7	1	0.97	0.97	
T = 550 K	2	0.61	0.58	
	3	0.73	0.73	
	4	0.69	0.67	
	5	0.70	0.70	
	6	0.70	0.70	

system as calculated by several methods and Auger data. The modified Williams and Nason model in the legend refers to a Williams and Nason broken-bond model (*20*) but modified in such a way to account for the fact that the bond energy of the surface atoms is different from bulk atom bond energies. Agreement of the multilayer model presented in this paper with the Auger data and other models is excellent.

Cu–Ni System

A good example of an alloy that exhibits endothermic mixing behavior is the Cu–Ni system. A graph of layer one versus bulk Cu composition is shown in Fig. 3 for the (111) surface, again assuming a regular solution activity model. Note that in this alloy

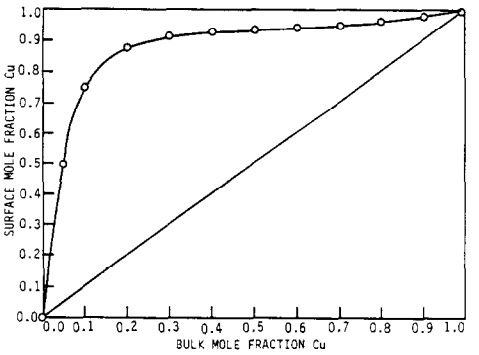

FIG. 3. First layer surface segregation of copper in the Cu–Ni system, T = 773 K, (111) surface.

the Cu is the segregating component. A typical composition depth profile for the Cu–Ni system is shown in Fig. 4. In contrast to the profile for Ag–Au, the endothermic mixing nature of the Cu–Ni system results in a profile that exhibits a monotonic decrease in Cu content as one gets further away from the surface. These results agree with previous predictions for this system obtained by using a different model (*31*).

Since the Cu–Ni alloy exhibits an asymmetric free energy of mixing curve, it is instructive to compare the results of surface segregation predictions by using the regular solution activity model (which assumes the free energy of mixing curve to be symmetric) with predictions using a three-suffix Margules model. The results of the surface segregation computations using the two different activity models are shown in Table 3 where they are compared with LEIS results

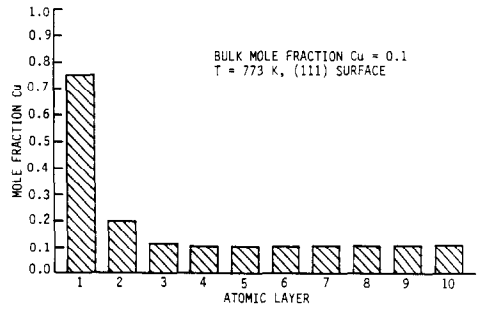

FIG. 4. Surface region composition depth profile for the Cu–Ni system.

TABLE 3

Comparison of Regular Solution and Margules Activity Models with LEIS and FIM Data

Layer	Mole fraction Ni		
	Regular solution	Margules	LEIS (47)[a]
Cu–Ni(111), T = 773 K			
1	0.07	0.10	0.04
2	0.30	0.38	
3	0.39	0.44	
4	0.44	0.47	
5	0.46	0.47	
6	0.47	0.48	
Bulk	0.48	0.48	0.48
Cu–Ni(111), T = 773 K			
1	0.12	0.13	0.12
2	0.58	0.53	
3	0.75	0.68	
4	0.79	0.75	
5	0.80	0.78	
6	0.80	0.79	
Bulk	0.80	0.80	0.80
Cu–Ni(111), T = 773 K			
1	0.22	0.19	0.21
2	0.78	0.73	
3	0.88	0.86	
4	0.89	0.88	
5	0.89	0.89	
6	0.89	0.89	
Bulk	0.89	0.89	0.89
			FIM (48)
Cu–Ni(111), T = 823 K			
1	0.58	0.45	0.46
2	0.93	0.91	
3	0.95	0.95	
4	0.95	0.95	
Bulk	0.95	0.95	0.95
			FIM (49)
Cu–Ni(111), T = 870 K			
1	0.935	0.924	0.511 + 0.075
2	0.990	0.989	
3	0.990	0.990	
4	0.990	0.990	
Bulk	0.990	0.990	0.990
Cu–Ni(111), T = 870 K			
1	0.585	0.463	0.236 ± 0.05
2	0.917	0.892	
3	0.937	0.934	
4	0.938	0.938	
5	0.938	0.938	
6	0.938	0.938	
Bulk	0.938	0.938	0.938
Cu–Ni(111), T = 870 K			
1	0.21	0.19	0.15 ± 0.05
2	0.66	0.61	
3	0.77	0.74	
4	0.80	0.78	
5	0.80	0.79	
6	0.80	0.80	
Bulk	0.80	0.80	0.80

[a] Polycrystalline sample.

of Brongersma *et al.* (*47*) and FIM data from Ng and McLane (*48*) and Sakurai *et al.* (*49*). Both the regular solution and Margules activity models agree well with the LEIS data; however, the Margules model shows better agreement with the FIM data than does the regular solution model.

Au–Ni System

The Au–Ni alloy was studied in order to gain insight into the effect of constituent size differences on surface segregation because these elements have significantly different lattice constants (3.52 Å for Ni and 4.08 Å for Au at 298 K). Surface segregation calculations were performed on a nickel-rich Au–Ni system by first assuming that the elements had equal lattice constants (equal to that of nickel) and then by allowing the lattice constants to differ. A regular solution model was assumed and no energetic variation in the mixing parameter was used; one could argue that the latter is a larger effect. The results of these calculations are given in Table 4 where comparison is made with Auger results from Williams and Boudart (*50*) and ISS results from Kelley *et al.* (*51*). One can see that the predicted surface segregation for Au is significantly higher at very dilute concentration when the size difference between the two elements is accounted for. Although there is significant disagreement between experiment and theory at a bulk gold mole fraction of 0.004, the experimental value of a first-layer gold concentration of 50% (at 1300 K) seems excessively high given such a low bulk content. The effect of size observed in this study is qualitatively what one would expect from strain energy considerations (*24, 52*) since, all else being equal, the strain energy will be lowered slightly if the larger solute atoms predominate at the surface.

Cu–Ni–Pt System

An example of predicted surface segregation behavior in a ternary alloy system may

TABLE 4

Predicted First Layer Compositions for the Au–Ni System

Layer	Mole fraction Au		
	Equal areas[a]	Unequal areas	Auger (50)[b]
Au–Ni(111), T = 1300 K			
1	0.052	0.093	0.50
2	0.004	0.004	
3	0.004	0.004	
4	0.004	0.004	
Bulk	0.004	0.004	0.004
Au–Ni(111), T = 1300 K			
1	0.49	0.70	0.70
2	0.052	0.066	
3	0.035	0.036	
4	0.035	0.035	
5	0.035	0.035	
Bulk	0.035	0.035	0.035
Au–Ni(111), T = 1300 K			
1	0.92	0.94	0.86
2	0.44	0.47	
3	0.28	0.29	
4	0.24	0.24	
5	0.23	0.23	
Bulk	0.23	0.23	0.23
			ISS (51)[b]
Au–Ni(111), T = 923 K			
1	0.61	0.87	0.88
2	0.02	0.03	
3	0.02	0.01	
4	0.01	0.01	
Bulk	0.01	0.01	0.01

Note. In one case, equal molar areas are assumed, while in the other case the actual, unequal, molar areas are used.

[a] Both molar areas taken to be equal to that of Ni.

[b] Surface orientation not specified.

be seen in Figs. 5 and 6. In Fig. 5 the surface composition of Ni is plotted versus bulk Ni composition. Note that with no Cu present, Ni segregates to the surface in the Ni–Pt alloy. However, as soon as Cu is added to the alloy, the surface becomes relatively depleted in Ni (due mainly to the comparatively low surface free energy of Cu). As more Cu is added, the relative surface depletion of Ni becomes greater. An example of a composition depth profile for the Cu–Ni–Pt system is given in Fig. 6. The fact that Cu–Pt and Ni–Pt interactions are exothermic in nature while Cu–Ni interactions are endothermic accounts for the rather complex behavior shown in this profile.

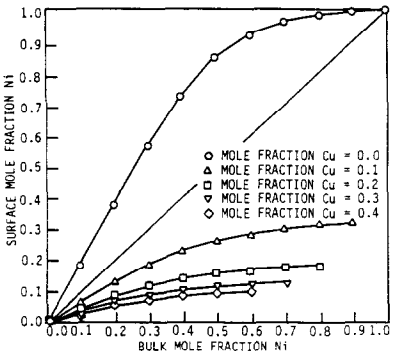

FIG. 5. First layer surface segregation of nickel in the Cu–Ni–Pt system, T = 1100 K, (100) surface.

The results presented in Fig. 6 suggest that subsurface composition variation may be quite complex in ternary alloys. The effect of subsurface composition on catalytic behavior of alloys is not yet known, but some possibilities may be suggested on the basis of the recent observations of subsurface adsorption sites. Reider and Stocker (*10*) have reported evidence for subsurface atomic hydrogen adsorption states on Cu(110) surfaces. Similar observations have been noted for hydrogen on Pd(110) (*7, 8*) and Nb(111). In addition, Lagos *et al.* (*11*) have suggested that subsurface adsorption states exist on platinum surfaces and that these weakly bonded, subsurface species play a role in H_2O formation and perhaps other hydrogenation reactions. The surface described by Fig. 6 has a first layer

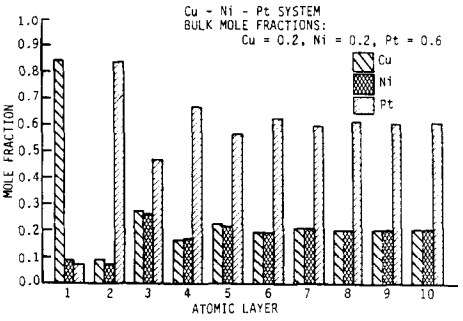

FIG. 6. Surface region composition depth profile for the Cu–Ni–Pt system, T = 1100 K, (100) surface.

that is nearly all copper and a second layer that is mostly platinum. If subsurface adsorption sites exist and if they play a significant role in catalysis one would expect that the ternary system would exhibit a catalytic behavior quite different from the analogous pure metal catalysts. Studies of multimetallic systems may allow parametric investigation of subsurface adsorption sites and other effects if the composition in the surface and near-surface region is known.

SUMMARY AND CONCLUSIONS

A model and computer algorithm for the prediction of surface segregation behavior in alloy systems has been developed in this work. The axioms of classical thermodynamics were used in the development of this model; indeed, the basis equation (Eq. (13)) of this model is thermodynamically rigorous. All major simplifying assumptions are based on nearest-neighbor-only interactions, which are quite reasonable for the systems studied. The chief advantages of this model and computer algorithm in comparison to previous models and methods are as follows:

- The variation of bond strength with coordination is automatically accounted for by surface free energy data that are incorporated into the model.
- The computer program allows for the incorporation of virtually any activity model.
- Size differences between elements are intrinsically accounted for.
- Systems with more than two components may be modeled.
- No adjustable parameters are needed.

Due to limitations in experimental data the model assumes that the mixing behavior is the same in the surface and bulk.

If properly used, the multilayer, multicomponent surface segregation model described in this paper can provide useful insights not only in the field of catalysis but also in other areas where knowledge of surface composition and behavior is important.

APPENDIX: DERIVATION OF EQ. (15) IN TEXT

Consider three atomic layers in the surface region labeled l, $l + 1$, and $l - 1$.

The expression for the surface activity may be derived by use of the following three-step procedure that parallels the one given in Ref. (*53*, pp. 173–175, 182–183):

1. Using simple bond-counting formulas, one can determine the configurational energy of layers l, $l - 1$, and $l + 1$.
2. Using the results from step 1, one can obtain an expression for the free energy of layer l.
3. Differentiating the free energy from step 2 with respect to component mole numbers, one can generate the expression for the surface chemical potential.

Step 1. The configurational energy due to interactions between layer l and $l - 1$ is given by

$$\underline{U}^{c}_{(l\leftrightarrow l-1)} = N_0 n Z_v [x^l_A x^{l-1}_A U_{AA} + x^l_B x^{l-1}_B U_{BB} + (x^l_A x^{l-1}_B + x^l_B x^{l-1}_A) U_{AB}], \quad \text{(A1)}$$

where n is the number of gram atoms present in a monolayer. Similarly, the configurational energy arising from interlayer interactions between layer l and $l + 1$ is given by

$$\underline{U}^{c}_{(l\leftrightarrow l+1)} = N_0 n Z_v [x^l_A x^{l+1}_A U_{AA} + x^l_B x^{l+1}_B U_{BB} + (x^l_A x^{l+1}_B + x^l_B x^{l+1}_A) U_{AB}]. \quad \text{(A2)}$$

The configurational energy due to intralayer interactions is

$$\underline{U}^{c}_{(l\leftrightarrow l)} = \tfrac{1}{2} N_0 n Z_L [(x^l_A)^2 U_{AA} + (x^l_B)^2 U_{BB} + 2 x^l_A x^l_B U_{AB}]. \quad \text{(A3)}$$

Configurational energy attributable to layer $l - 1$ arising from interactions between this layer and layer $l - 2$ (if present) is given by

$$\underline{U}^{c}_{(l-1\leftrightarrow l-2)} = \tfrac{1}{2} N_0 n Z_v [x^{l-1}_A x^{l-2}_A U_{AA} + x^{l-1}_B x^{l-2}_B U_{BB} + (x^{l-1}_A x^{l-2}_B + x^{l-1}_B x^{l-2}_A) U_{AA}].$$

However, if one makes the assumption that $x^{l-1} = x^{l-2}$, the above expression reduces to

$$\underline{U}^{c}_{(l-1\leftrightarrow l-2)} \simeq \tfrac{1}{2}N_0nZ_v[(x_A^{l-1})^2U_{AA} + (x_B^{l-1})^2U_{BB} + 2x_A^{l-1}x_B^{l-1}U_{AB}]. \quad (A4)$$

This assumption introduces very little error in determining the total configurational energy due to layers l, $l-1$, and $l+1$. For example, in typical binary alloy systems such as Ag–Au and Cu–Ni, this error is less than one percent. If we use a similar argument, the analogous term for layer $l+1$ is

$$\underline{U}^{c}_{(l+1\leftrightarrow l+2)} \simeq \tfrac{1}{2}N_0nZ_v[(x_A^{l+1})^2U_{AA} + (x_B^{l+1})^2U_{BB} + 2x_A^{l+1}x_B^{l+1}U_{AB}]. \quad (A5)$$

The lateral contributions from layers $l-1$ and $l+1$ to the total configurational energy are, respectively,

$$\underline{U}^{c}_{(l-1\leftrightarrow l-1)} = \tfrac{1}{2}N_0nZ_L[(x_A^{l-1})^2U_{AA} + (x_B^{l-1})^2U_{BB} + 2x_A^{l-1}x_B^{l-1}U_{AB}] \quad (A6)$$

$$\underline{U}^{c}_{(l+1\leftrightarrow l+1)} = \tfrac{1}{2}N_0nZ_L[(x_A^{l+1})^2U_{AA} + (x_B^{l+1})^2U_{BB} + 2x_A^{l+1}x_B^{l+1}U_{AB}]. \quad (A7)$$

Adding expressions (A1) through (A7) and rearranging give the total configurational energy of the three layers:

$$\underline{U}^{c}_{(\text{total})} = \tfrac{1}{2}N_0nZ[x_A^{l-1}U_{AA} + x_B^{l-1}U_{BB}] + nqx_A^{l-1}x_B^{l-1} + \tfrac{1}{2}N_0nZ(x_A^{l+1}U_{AA} + x_B^{l+1}U_{BB}) + nqx_A^{l+1}x_B^{l+1} + \tfrac{1}{2}N_0nZ(x_A^{l}U_{AA} + x_B^{l}U_{BB}) + npqx_A^{l}x_B^{l} + nvq(x_A^{l}x_B^{l-1} + x_B^{l}x_A^{l-1} + x_A^{l}x_B^{l+1} + x_B^{l}x_A^{l+1} - x_A^{l-1}x_B^{l-1} - x_A^{l+1}x_B^{l+1}), \quad (A8)$$

where $q = N_0Z[U_{AB} - \frac{1}{2}(U_{AA} + U_{BB})]$, $p = Z_L/Z$, and $v = Z_v/Z$.

Step 2. Since the configurational energy for a bulk system with n total moles of components A and B is given by

$$\underline{U}^{c}_{(\text{bulk})} = \tfrac{1}{2}N_0nZ(x_AU_{AA} + x_BU_{BB}) + nqx_Ax_B$$

one can see that the first two terms on the right-hand side of Eq. (A8) represent the configurational energy of layer $l-1$ if that layer is assumed to be in the bulk. Similarly, the next two terms represent the bulk configurational energy of layer $l+1$. Thus, the contribution of layer l to the configurational energy is

$$\underline{U}^{c}_{(l)} = \tfrac{1}{2}N_0nZ(x_A^{l}U_{AA} + x_B^{l}U_{BB}) + npqx_A^{l}x_B^{l} + nvq(x_A^{l}x_B^{l-1} + x_B^{l}x_A^{l-1} + x_A^{l}x_B^{l+1} + x_B^{l}x_A^{l+1} - x_A^{l-1}x_B^{l-1} - x_A^{l+1}x_B^{l+1}). \quad (A9)$$

The terms in Eq. (A9) which originate from mixing effects are those terms containing q. Knowing this, one can immediately write the mixing energy component $\underline{E}^{M}$,

$$\underline{E}^{M} = qpnx_A^{l}x_B^{l} + nvq(x_A^{l}x_B^{l-1} + x_B^{l}x_A^{l-1} + x_A^{l}x_B^{l+1} + x_B^{l}x_A^{l+1} - x_A^{l-1}x_B^{l-1} - x_A^{l+1}x_B^{l+1}).$$

The above expression can be rearranged to yield

$$\underline{E}^{M} = n_A^{l}q(x_B^{l})^2 + n_B^{l}q(x_A^{l})^2 + npq[(x_B^{l} - x_B^{l-1})^2 + (x_B^{l} - x_B^{l+1})^2], \quad (A10)$$

where n_A^{l} and n_B^{l} represent the number of moles of components A and B in layer l.

Writing the Helmholz free energy of layer l as the sum of ideal and mixing parts gives

$$\underline{F}_l = n_A^{l}(\mu_A^{0,l} + RT\ln x_A^{l}) + n_B^{l}(\mu_B^{0,l} + RT\ln x_B^{l}) + \underline{E}^{M}. \quad (A11)$$

Substituting for $\underline{E}^{M}$, using Eq. (A10), and rearranging lead to the expression

$$\underline{F}_l = n_A^{l}[\mu_A^{0,l} + RT\ln x_A^{l} + q(x_B^{l})^2] + n_B^{l}[\mu_B^{0,l} + RT\ln x_B^{l} + q(x_A^{l})^2] + nvq[(x_B^{l} - x_B^{l-1})^2 + (x_B^{l} - x_B^{l+1})^2]. \quad (A12)$$

Step 3. Differentiating Eq. (A12) with respect to n^{l} and rearranging give

$$\left(\frac{\partial \underline{F}^l}{\partial n_A^l}\right)_{T,\underline{V}^l,n_B^l} - \mu_A^{0,l} = qp(x_B^l)^2 + qv[(x_B^{l-1})^2 + (x_B^{l+1})^2]. \quad \text{(A13)}$$

But since

$$\left(\frac{\partial \underline{F}^l}{\partial n_A^l}\right)_{T,\underline{V}^l,n_B^l} - \mu_A^{0,l} = RT \ln a_A^l \quad \text{(A14)}$$

one can substitute (A14) into (A13) to get

$$RT \ln a_A^l = qp(x_B^l)^2 + qv[(x_B^{l-1})^2 + (x_B^{l+1})^2]. \quad \text{(A15)}$$

Substituting $N_0\omega_{AB}Z$ back in for q yields the desired expression

$$RT \ln a_A^l = \frac{N_0\omega_{AB}}{Z}\{Z_L(x_B^l)^2 + Z_v[(x_B^{l-1})^2 + (x_B^{l+1})^2]\}. \quad \text{(A16)}$$

ACKNOWLEDGMENTS

This material is based upon work supported by the National Science Foundation under Grant CPE-8307959. The support of the Engineering Research Institute at Iowa State University is also acknowledged.

REFERENCES

1. Balandin, A. A., *Z. Phys. Chem. B* **2,** 289 (1929).
2. Kobozev, N. J. *Acta Physicochim. URSS* **9,** 805 (1938).
3. Ponec, V., and Sachtler, W. M. H., *in* "Proceedings, 5th International Congress on Catalysis, Palm Beach, 1977" (J. W. Hightower, Ed.), p. 645. American Elsevier, New York, 1972.
4. Sinfelt, J. H., "Bimetallic Catalysts, Discoveries, Concepts, and Applications." Wiley, New York, 1983, and references therein.
5. Ricter, L., Bader, S. D., and Brodsky, M. B., *J. Vac. Sci. Technol.* **18,** 578 (1981).
6. Houston, J. E., Peden, C. H. F., Feibelman, P. J., and Hamann, D. R., *Phys. Rev. Lett.* **56,** 375 (1986).
7. Rieder, K. H., Baumberger, M., and Stocker, W., *Phys. Rev. Lett.* **51,** 1799 (1983).
8. Behm, R. J., Penka, V., Cattania, M. G., Christmann, K., and Ertl, G., *J. Chem. Phys.* **78,** 7486 (1983).
9. Ying, L., Erskine, J. L., and Diebold, A. C., *Phys. Rev. B* **34,** 5951 (1986).
10. Rieder, K. H., and Stocker, W., *Phys. Rev. Lett.* **57,** 2548 (1986).
11. Lagos, M., Ramirez, R., and Schuller, I. K., *Phys. Rev. B* **38,** 10042 (1988).
12. Gibbs, J. W., "Collected Works," Vol. I. Yale Univ. Press, New Haven, CT, 1948.
13. Butler, J. A. V., *Proc. R. Soc. London* **135,** 348 (1932).
14. Schuchowitzky, A., *Acta Physicochim. URSS* **19**(2–3), 176 (1944).
15. Guggenheim, E. A., *Trans. Faraday Soc.* **41,** 150 (1945).
16. Defay, R., and Prigogine, I., *Trans. Faraday Soc.* **46,** 199 (1950).
17. Ono, S., *Mem. Fac. Eng. Kyushu Univ.* **10**(4), 213 (1947). Ono, S., *Mem. Fac. Eng. Kyushu Univ.* **12,** 1 (1950). Ono, S., and Kondo, S., *Handb. Physik* **10,** 134 (1960).
18. Mezey, L. Z., and Giber, J., *Surf. Sci.* **117,** 220 (1982); *Japan. J. Appl. Phys.* **21**(11), 1569 (1982); Mezey, L. Z., *Surf. Sci.* **162,** 510 (1985); Mezey, L. Z., and Giber, J., *Surf. Sci.* **162,** 514 (1985).
19. Kelley, M. J., *J. Catal.* **57,** 113 (1979).
20. Williams, F. C., and Nason, D., *Surf. Sci.* **45,** 377 (1974).
21. Kumar, V., Kumar, D., and Joshi, S., *Phys. Rev. B* **19**(4), 1954 (1979).
22. Cheng, Y., Wu, C., and Chiang, R., *Phys. Rev. B* **32,** 4224 (1985).
23. Moran-Lopez, J., and Falicov, L., *Phys. Rev. B* **18**(6), 2549 (1978).
24. Wynblatt, P., and Ku, R., *Surf. Sci.* **65,** 511 (1977).
25. Gijzeman, O., *Surf. Sci.* **150,** 1 (1985).
26. Lambin, P., and Gaspard, J., *J. Phys. F* **10,** 2413 (1980).
27. Eckert, C. A., and Prausnitz, J. M., *AIChE J.* **10**(5), 677 (1964).
28. Burton, J. J., Hyman, E., and Fedak, D. G., *J. Catal.* **37,** 106 (1975).
29. Tomanek, D., Aligia, A., and Balseiro, C., *Phys. Rev. B* **32**(8), 5051 (1985).
30. King, T. S., and Donnelly, R. G., *Surf. Sci.* **141,** 417 (1984).
31. Donnelly, R. G., and King, T. S., *Surf. Sci.* **74,** 89 (1978).
32. Lundberg, M., *Phys. Rev. B* **36**(9), 4692 (1987).
33. Foiles, S. M., *Phys. Rev. B* **32,** 7685 (1985).
34. Modell, M., and Reid, R. C., "Thermodynamics and Its Applications." Prentice-Hall, Englewood Cliffs, NJ, 1983.
35. Swalin, R. A., "Thermodynamics of Solids." Wiley, New York, 1972.
36. Maitland, G. C., Rigby, M., Smith, B. E., and Wakeham, W. A., "Intermolecular Forces." Clarendon Press, Oxford, 1981.
37. Tsai, N. H., Abraham, F. F., and Pound, G. M., *Surf. Sci.* **77,** 465 (1978).
38. Guggenheim, E. A., "Mixtures." Oxford Univ. Press, Amen House, London, 1952.
39. Pearson, W. B., "A Handbook of Lattice Spacings and Structures of Metals and Alloys." Pergamon, London, 1958.
40. Tyson, W. R., *Canad. Metall. Q* **14**(4), 307 (1975).

41. Murr, L. E., "Interfacial Phenomena in Metals and Alloys." Addison–Wesley, Reading, MA, 1975.
42. Hultgren, R., Desai, P. D., Hawkins, D. T., Gleiser, M., and Kelley, K. K., "Selected Values of the Thermodynamic Properties of Binary Alloys." American Society for Metals, Metals Park, OH, 1973.
43. Hultgren, R., Desai, P. D., Hawkins, D. T., Gleiser, M., Kelley, K. K., and Wagman, D. D., "Selected Values of the Thermodynamic Properties of the Elements." American Society for Metals, Metals Park, OH, 1973.
44. Kittel, C., "Introduction to Solid State Physics," 6th ed. Wiley, New York, 1986.
45. Miedema, A. R., *Philips Tech. Rev.* **36**(8), 217 (1976).
46. King, T. S., and Donnelly, R. G., *Surf. Sci.* **151,** 374 (1985).
47. Brongersma, H. H., Sparnay, M. J., and Buck, T. M., *Surf. Sci.* **71,** 657 (1978).
48. Ng, Y. S., and McLane, S. B., Jr., *Surf. Sci.* **84,** 31 (1979).
49. Sakurai, T., Hashizume, T., Kobayashi, A., Sakai, A., Hyodo, S., Kuk, Y., and Pickering, H. W., *Phys. Rev. B* **34**(12), 8379 (1986).
50. Williams, F. L., and Boudart, M., *J. Catal.* **30,** 438 (1973).
51. Kelley, M. J., Gilmour, P. W., and Swartzfager, D. G., *J. Vac. Sci. Technol.* **17**(2), 634 (1980).
52. McLean, D., "Grain Boundaries in Metals." Oxford Univ. Press, London, 1957.
53. Defay, R., and Prigogine, I., "Surface Tension and Adsorption." Longmans, London, 1966.